MSUHEP–21111 UCLA/02/TEP/34 SLAC–PUB–9573

arXiv:hep-ph/0211216v1 14 Nov 2002

The Di-Photon Background to a Light Higgs Boson at the LHC

Zvi Bern,[a*] Lance Dixon[b†] and Carl Schmidt[c‡]

[a]Department of Physics and Astronomy
UCLA, Los Angeles, CA 90095-1547, USA

[b]Stanford Linear Accelerator Center
Stanford University, Stanford, CA 94309, USA

[c]Department of Physics and Astronomy
Michigan State University, East Lansing, MI 48824, USA

Recent years have seen a significant advance in our ability to calculate two-loop matrix elements. In this talk we describe an application of this breakthrough to improve our understanding of the background to the search for a light Higgs boson at the LHC. In particular, we focus on the QCD corrections to the gluon fusion subprocess $gg \to \gamma\gamma$, which forms an important component of the background in the di-photon channel. We find that the K factor for this subprocess is significantly smaller than estimated previously.

1. INTRODUCTION

Many of the talks at this conference described the recent wonderful advances in two-loop perturbative calculations (see e.g. refs. [1–3] and references therein). Here we outline the application of this breakthrough to a phenomenological study [4] of the background to the search for a Higgs boson at the LHC in the di-photon mode. In a complementary talk at this conference, Abilio De Freitas [2] described the calculation [5] of the two-loop matrix elements for gluon fusion into a photon pair used in this study.

Arguably, the most pressing problem in particle physics today is the origin of electroweak symmetry breaking. Collider experiments over the next decade should shed considerable light on this by searching for the Higgs boson and measuring its physical properties. No matter what new physics lies beyond the Standard Model (SM), measurements of the Higgs sector parameters will likely provide crucial clues to its structure.

There are a few reasons to suspect that the mass of at least one Higgs particle is quite light. Most strikingly, the SM Higgs boson mass is bounded from above by precision electroweak measurements, $m_H \lesssim 200$ GeV at 95% CL. There are also hints of a signal in the direct search in $e^+e^- \to HZ$ at LEP2, near the lower mass limit of 114 GeV. In the minimal supersymmetric theory the lightest Higgs mass is $\lesssim 135$ GeV.

For $m_H \lesssim 140$ GeV, the preferred search mode at the LHC involves Higgs production via gluon fusion, followed by the rare decay into a pair of photons [6]. (For a discussion of other useful modes see *e.g.* ref. [7].) Although the branching ratio is tiny, the di-photon mode is relatively clean due to the excellent mass resolution of the LHC detectors, which will allow the background to be measured experimentally and subtracted from a putative signal [8,9]. Nevertheless, it is still important to have robust theoretical predictions in order to systematically study the dependence of the signal relative to the background to optimize Higgs search strategies. Since it will take about two years of running at the LHC to extract the $\gamma\gamma$ signal from the background, there is good motivation for improving search strategies.

Given the intense theoretical effort that has

*Presenter at RADCOR 2002/Loops and Legs in Quantum Field Theory (September 2002, Kloster Banz, Germany). Research supported by the US Department of Energy under grant DE-FG03-91ER40662.
†Research supported by the US Department of Energy under contract DE-AC03-76SF00515.
‡Research supported by the US National Science Foundation under grant PHY-0070443.

gone into two-loop calculations with more than a single kinematic variable, it is obviously beneficial to have concrete examples where the new advances have already impacted phenomenology. The background to Higgs decay discussed here is one such example. Another recent example was presented in the talk by Anastasiou [3], where an exact calculation [10] of next-to-next-to-leading-order (NNLO) inclusive Higgs production [11] was described. The choice of Higgs physics as among the first applications stems from both its importance for the future of particle physics as well as the relative simplicity of the infrared divergences encountered in the calculations. Once algorithms are set up for dealing more generally with NNLO infrared divergent phase space many more applications will certainly appear [1].

2. THE DI-PHOTON BACKGROUND

The background to the Higgs search in the di-photon mode consists of two pieces. The 'reducible' background arises when photons are faked by jets, or more generally by hadrons, especially π^0s. This background can be efficiently suppressed by photon isolation cuts, where events are rejected based on the hadronic energy near the photons [8,9,12–14]. The 'irreducible' background, which we focus on here, arises from the underlying QCD process where quarks emit photons either directly or through fragmentation.

The process $pp \to \gamma\gamma X$ proceeds at lowest order via quark annihilation, $q\bar{q} \to \gamma\gamma$. The NLO corrections to this subprocess have been incorporated into a number of Monte Carlo programs [15,16]; the most up-to-date, `DIPHOX` [17], also includes fragmentation contributions.

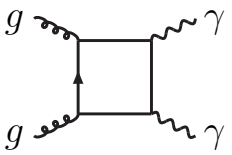

Figure 1. A leading order diagram contributing to gluon fusion into two photons.

The largest of the contributions that have not yet been incorporated into `DIPHOX` are the NLO corrections to gluon fusion into a di-photon pair. Although the one-loop gluon fusion contribution (fig. 1) is formally of higher order in the QCD coupling than the tree-level process $q\bar{q} \to \gamma\gamma$, it is enhanced by the large gluon distribution in the proton at small x, so that it becomes numerically comparable [15–19]. To reduce the uncertainty on the total $\gamma\gamma$ production rate, a calculation of the $gg \to \gamma\gamma$ subprocess at its next-to-leading-order is required, even though it is formally N^{3}LO as far as the whole process $pp \to \gamma\gamma X$ is concerned. A number of other α_s^2 and α_s^3 contributions should eventually also be included, although they are expected to be less significant [4].

3. GLUON FUSION AT NLO

3.1. Matrix Elements and Singularities

The NLO correction to gluon fusion involves diagrams of the type shown in fig. 2. The two-loop virtual contributions (a) were recently computed [5], as summarized in the talk by De Freitas [2]. The real emission contributions (b) are obtained from a permutation sum [16] over contributions to the one-loop five-gluon amplitude [20].

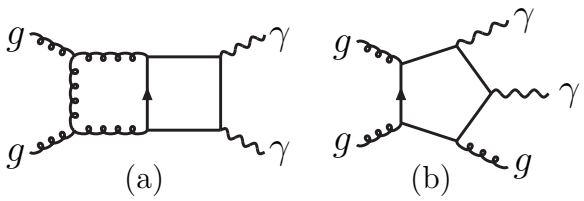

Figure 2. Sample NLO diagrams contributing to gluon fusion into two photons: (a) virtual and (b) real emission contributions.

Both the virtual and real corrections have been evaluated for zero quark mass. In the range of di-photon invariant masses $M_{\gamma\gamma}$ relevant for the light Higgs search (90–150 GeV) this is an excellent approximation: the masses of the five light quarks are negligible, while the top quark contribution is tiny for $M_{\gamma\gamma} \ll 2m_t \approx 350$ GeV.

In order to obtain a prediction for a physical cross section, virtual and real corrections must be combined to cancel the infrared divergences appearing in each term. Because $gg \to \gamma\gamma$ vanishes at tree-level, the divergences encountered in the NLO corrections to $gg \to \gamma\gamma X$ have the structure of a typical NLO QCD calculation, even though two-loop matrix elements are involved. We could therefore employ the dipole formalism [21].

3.2. Photon Isolation

To reduce fragmentation contributions and also to reject the reducible background, photon isolation criteria are imposed. There are two standard ways to do this: (a) *standard* cone isolation where the amount of transverse hadronic energy $E_{\rm T}$ in a cone of radius $R = \sqrt{(\Delta\eta)^2 + (\Delta\phi)^2}$ must be less than $E_{\rm T\,max}$ and (b) *smooth* cone isolation [22] where the amount of transverse hadronic energy $E_{\rm T}$ in *all* cones of radius r with $r < R$ must be less than a given function, for example:

$$E_{\rm T\,max}(r) \equiv p_{\rm T}(\gamma)\,\epsilon \left(\frac{1-\cos r}{1-\cos R}\right). \qquad (1)$$

The smooth cone is preferred theoretically because it eliminates the fragmentation contributions. However, it may be problematic experimentally, due to the finite width of a photon's electromagnetic shower and the relatively large granularity of the LHC calorimeters [13]. We have implemented both isolation algorithms. For the standard cone we use `DIPHOX` [17] to obtain all contributions except the gluon fusion ones; for the smooth cone we constructed an independent NLO program for all pieces.

4. RESULTS FOR DI-PHOTON BACKGROUND

Figure 3 illustrates the shift in the total NLO $pp \to \gamma\gamma X$ production rate, for the case of standard cone isolation, due to the gluon fusion subprocess. The lower curve in the plot is obtained from `DIPHOX` [17], incorporating the gluon fusion subprocess only at its leading order. The upper curve includes the NLO contributions to gluon fusion. The increase in the total irreducible $\gamma\gamma$ background which results from replacing the LO gluon fusion quark box by the NLO computation

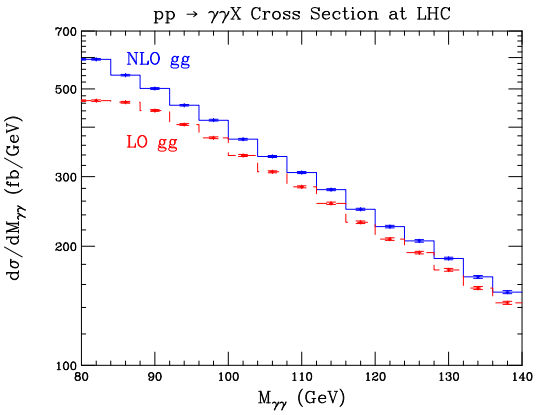

Figure 3. Total $pp \to \gamma\gamma X$ production at NLO, including NLO $q\bar{q} \to \gamma\gamma$ and fragmentation contributions, with the gluon fusion subprocess treated at LO (lower) and at NLO (upper). In these plots the renormalization and factorization scales are $\mu_R = \mu_F = M_{\gamma\gamma}/2$, using MRST99 set 2 partons. A standard photon isolation criterion is used with $R = 0.4$, $E_{\rm T\,max} = 15$ GeV.

is a relatively modest one, except at the lowest invariant masses which are not relevant for SM Higgs searches. For the most interesting mass range 115 GeV $< m_H <$ 140 GeV, the overall effect on the square root of the background is under 5%. Thus, this subprocess can be considered to be under adequate theoretical control. A more detailed discussion of these results may be found in ref. [4].

Prior to the NLO calculation, some experimental studies had used the K factor (ratio of NLO over LO cross section) for Higgs production by gluon fusion to estimate the K factor for $gg \to \gamma\gamma$. After all, both $gg \to H$ and $gg \to \gamma\gamma$ produce a colorless system from a gg initial state. Actually, the background K factor is significantly smaller, only about 65% of the signal K factor for a broad range of Higgs masses. This difference is partially due to a short-distance renormalization contribution that only affects the Higgs production process. The remainder can be traced to the heaviness of the top quark in the Higgs production loop diagram: the background process involves light quarks and is "softer" when an extra

gluon attaches to the loop [4].

5. STATISTICAL SIGNIFICANCE OF HIGGS SIGNAL AND OUTLOOK

To study the statistical significance of the signal, we implemented the gluon fusion production of the SM Higgs boson at NLO [23,24], followed by decay to $\gamma\gamma$, with a branching ratio obtained from the program `HDECAY` [25]. As is standard for a light Higgs boson, we work in the heavy top quark limit, for which an effective Hgg vertex [26] suffices to describe the production process at low Higgs transverse momenta.

The interference between the Higgs signal and background is rather tiny, mainly because the Higgs resonance in this mass range is extremely sharp, but also because of properties of the background amplitudes [4]. Thus one can consider the signal and background cross sections separately.

5.1. Effects of Varying Photon Isolation

Armed with a reliable theoretical calculation, one can systematically study the effects on both signal and background of varying the photon isolation criteria. One can also search for the best kinematic cuts and variable choices for enhancing the signal over the background.

For example, Figure 4 shows the dependence of the $pp \to \gamma\gamma X$ production rate at the LHC on the parameters of the smooth isolation cone criterion [4]. As the isolation becomes more severe, *i.e.* R is increased or ϵ is decreased, the direct $pp \to \gamma\gamma X$ background becomes more suppressed. The large sensitivity to these parameters is due to the $q\gamma$ collinear singularity in the NLO $q\bar{q} \to \gamma\gamma X$ cross section. Since the QCD radiation in Higgs production has no such singularity, it should be uncorrelated with the photon directions, and so the signal is less sensitive to the isolation criterion.

A better way to suppress the QCD background is with a jet veto. At the NLO parton level, at least for direct processes, a jet veto corresponds closely to increasing the cone size. However, transverse energy can be forbidden into a smaller area (the jet cone size), for the same amount of suppression at NLO. Hence the jet veto should be better behaved theoretically. It should also have

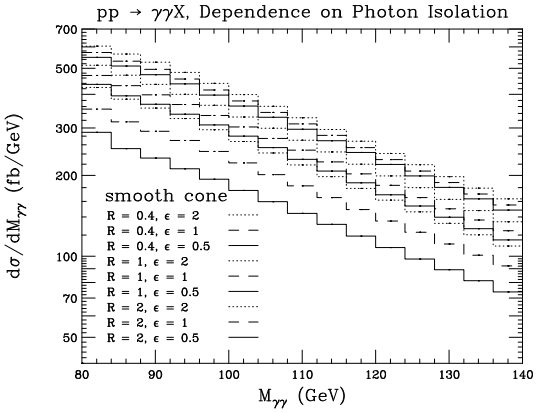

Figure 4. Dependence of $pp \to \gamma\gamma X$ at the LHC on photon isolation cuts, for a set of smooth cone isolation parameters, R and ϵ. All plots are for MRST99 set 2 partons, and $\mu_R = \mu_F = 0.5 M_{\gamma\gamma}$.

significantly better experimental properties since less signal is lost due to detector noise, overlapping events, *etc.*

In either of these cases, even though the background falls significantly, it turns out that $S/\sqrt{B}$ is rather insensitive to the tighter cuts [4]. One can improve the situation slightly by taking into account information about the rapidity difference between the two photons [4]. It also may be possible to find better variables characterizing the hadronic energy flow in the events, to reduce the number of signal events cut out.

Studies making use of hadronic energy flow would need to be carried out with a more realistic simulation than the parton-level one outlined here. In particular, effects of instrumental noise and overlapping events should be included [13]. It would also be very important to include a detailed study of the reducible π^0 background contributions [12–14]. Finally, other NNLO contributions could be added as they become available.

The improved calculation of the di-photon background to Higgs decay at the LHC described in this talk is the first collider physics application of the new two-loop QCD amplitudes depending on more than a single kinematic variable. In the near future, many more phenomenological applications should be forthcoming.

REFERENCES

1. E.W.N. Glover, in these proceedings; T. Gehrmann, in these proceedings, hep-ph/0210157; G. Heinrich; in these proceedings; E. Remiddi, in these proceedings; S. Moch, P. Uwer, S. Weinzierl, in these proceedings and hep-ph/0210009. V. A. Smirnov, in these proceedings, hep-ph/0209295.
2. Z. Bern, A. De Freitas and L. Dixon, in these proceedings.
3. C. Anastasiou and K. Melnikov, in these proceedings.
4. Z. Bern, L. Dixon and C. Schmidt, Phys. Rev. D **66**, 074018 (2002) [hep-ph/0206194].
5. Z. Bern, A. De Freitas and L.J. Dixon, JHEP **0109**, 037 (2001) [hep-ph/0109078].
6. J.F. Gunion, P. Kalyniak, M. Soldate and P. Galison, Phys. Rev. D **34**, 101 (1986); J.F. Gunion, G.L. Kane and J. Wudka, Nucl. Phys. B **299**, 231 (1988).
7. D. Rainwater, M. Spira and D. Zeppenfeld, hep-ph/0203187.
8. ATLAS collaboration technical design report, vol. 2, report CERN/LHCC 99-15, ATLAS-TDR-15.
9. CMS collaboration, electromagnetic calorimeter technical design report, report CERN/LHCC 97-33, CMS-TDR-4.
10. C. Anastasiou and K. Melnikov, hep-ph/0207004.
11. R.V. Harlander and W.B. Kilgore, Phys. Rev. Lett. **88**, 201801 (2002) [hep-ph/0201206]; R. Harlander, in these proceedings.
12. V. Tisserand, "The Higgs to two photon decay in the ATLAS detector," LAL 96-92; Ph.D. thesis, LAL 97-01.
13. M. Wielers, "Isolation of photons," report ATL-PHYS-2002-004.
14. T. Binoth, J.P. Guillet, E. Pilon and M. Werlen, hep-ph/0203064.
15. E.L. Berger, E. Braaten and R.D. Field, Nucl. Phys. B **239**, 52 (1984); P. Aurenche, A. Douiri, R. Baier, M. Fontannaz and D. Schiff, Z. Phys. C **29**, 459 (1985); B. Bailey, J.F. Owens and J. Ohnemus, Phys. Rev. D **46**, 2018 (1992); B. Bailey and J.F. Owens, Phys. Rev. D **47**, 2735 (1993); B. Bailey and D. Graudenz, Phys. Rev. D **49**, 1486 (1994) [hep-ph/9307368]; C. Balazs, E.L. Berger, S. Mrenna and C.-P. Yuan, Phys. Rev. D **57**, 6934 (1998) [hep-ph/9712471]; C. Balazs and C.-P. Yuan, Phys. Rev. D **59**, 114007 (1999) [Erratum-ibid. D **63**, 059902 (1999)] [hep-ph/9810319]; T. Binoth, J.P. Guillet, E. Pilon and M. Werlen, Phys. Rev. D **63**, 114016 (2001) [hep-ph/0012191]; T. Binoth, hep-ph/0005194.
16. D. de Florian and Z. Kunszt, Phys. Lett. B **460**, 184 (1999) [hep-ph/9905283]; C. Balazs, P. Nadolsky, C. Schmidt and C.-P. Yuan, Phys. Lett. B **489**, 157 (2000) [hep-ph/9905551].
17. T. Binoth, J.P. Guillet, E. Pilon and M. Werlen, Eur. Phys. J. C **16**, 311 (2000) [hep-ph/9911340].
18. R.K. Ellis, I. Hinchliffe, M. Soldate and J.J. van der Bij, Nucl. Phys. B **297**, 221 (1988).
19. L. Ametller, E. Gava, N. Paver and D. Treleani, Phys. Rev. D **32**, 1699 (1985); D.A. Dicus and S.S.D. Willenbrock, Phys. Rev. D **37**, 1801 (1988).
20. Z. Bern, L. Dixon and D.A. Kosower, Phys. Rev. Lett. **70**, 2677 (1993) [hep-ph/9302280].
21. S. Catani and M.H. Seymour, Nucl. Phys. B **485**, 291 (1997) [Erratum-ibid. B **510**, 503 (1997)] [hep-ph/9605323].
22. S. Frixione, Phys. Lett. B **429**, 369 (1998) [hep-ph/9801442].
23. A. Djouadi, M. Spira and P.M. Zerwas, Phys. Lett. B **264**, 440 (1991); S. Dawson, Nucl. Phys. B **359**, 283 (1991); M. Spira, A. Djouadi, D. Graudenz and P.M. Zerwas, Nucl. Phys. B **453**, 17 (1995)[hep-ph/9504378].
24. M. Kramer, E. Laenen and M. Spira, Nucl. Phys. B **511**, 523 (1998)[hep-ph/9611272].
25. A. Djouadi, J. Kalinowski and M. Spira, Comput. Phys. Commun. **108**, 56 (1998) [hep-ph/9704448].
26. J.R. Ellis, M.K. Gaillard and D.V. Nanopoulos, Nucl. Phys. B **106**, 292 (1976); M.A. Shifman, A.I. Vainshtein, M.B. Voloshin and V.I. Zakharov, Sov. J. Nucl. Phys. **30**, 711 (1979) [Yad. Fiz. **30**, 1368 (1979)].